Radiation Physics and Chemistry 107 (2015) 59–64

Contents lists available at ScienceDirect

Radiation Physics and Chemistry

journal homepage: www.elsevier.com/locate/radphyschem

K shell parameters of some lanthanide elements using bremsstrahlung

K.M. Niranjana, N.M. Badiger *

Department of Physics, Karnatak University, Dharwad 580 003, India

HIGHLIGHTS

- Bremsstrahlung attenuation in Tb and Ho targets is measured.
- At K edge a sharp decrease in intensity is used to determine the K shell parameters.
- The K x-ray photons appear just below the K edge hinders the precise measurement.
- This hindrance is avoided using monochromatic gamma source.
- Measured values are compared with those obtained from FFAST tabulations.

ARTICLE INFO

Article history:
Received 30 April 2014
Received in revised form
28 August 2014
Accepted 30 September 2014
Available online 5 October 2014

Keywords:
K edge
K x-rays
Beta source
External bremsstrahlung
K shell photoelectric parameters

ABSTRACT

The spectrum of external bremsstrahlung (EB) transmitted through Tb and Ho is measured using a HPGe detector spectrometer. A sudden drop in transmitted intensity at K shell binding energy has been used to determine the K shell photoelectric parameters. The unwanted characteristic K x-ray photons generated just below the K edge has been avoided by carrying out a separate experiment in the same geometry. The measured values of K shell parameters have been compared with FFAST values.

1. Introduction

The K shell binding energies of lanthanides will be in the range of 38–64 keV. To measure the K shell binding energy of these elements one has to measure the mass attenuation coefficient at various energies around the K shell binding energy. A plot of mass attenuation coefficient versus photon energy gives a saw tooth structure; the sudden increase in mass attenuation coefficient is attributed to the involvement of K shell electrons in photoelectric absorption process. In other words, by knowing this saw tooth structure one can determine not only K shell binding energy but also other K shell photoelectric parameters such as K shell photoelectric cross-section at K edge, jump ratio, jump factor and Davisson–Kirchner ratio. The accurate values of these parameters are needed in understanding not only photo-absorption process but also in characterizing the materials. Such type of saw tooth structure for various elements and compounds were obtained by various authors by adopting different techniques. For instance by x-ray photon attenuation from a x-ray tube, gamma ray attenuation (Mallikarjuna et al., 2002), attenuation of Compton scattered photons (Ayala and Mainardi, 1996), attenuation of synchrotron radiation (Tran et al., 2005), attenuation of characteristic K X-ray photons (Çevik et al., 2006; Niranjana et al., 2013), attenuation of EB radiation from a β-ray source (Nayak and Badiger, 2006a, 2006b) and x-ray fluorescence measurements (Ertugrul et al., 2002; Bennal and Badiger, 2007).

One of the simple and novel methods to measure the K shell photoelectric parameters is the bremsstrahlung attenuation method. In this method a continuous bremsstrahlung spectrum is allowed to transmit through a target whose K shell parameters are to be determined. It is striking to note that in the recorded transmitted spectrum a sudden drop in intensity is observed at K shell binding energy of the target. In fact we have recently used this technique to understand effect of chemical environment on K shell binding energy of Ag and Sn (Niranjana et al., 2014).

In the present experiment we have shown that the K shell photoelectric parameters of Tb and Ho can be measured using the bremsstrahlung attenuation method. In this present method we

* Corresponding author.
E-mail addresses: nagappa123@yahoo.co.in, nbadiger@gmail.com (N.M. Badiger).

http://dx.doi.org/10.1016/j.radphyschem.2014.09.013
0969-806X/

have taken into account the presence of characteristic $K\beta_1'$ and $K\beta_2'$ x-ray photons. To account for the contribution of K β_1' and $K\beta_2'$ x-ray peaks, appearing just below the K edge, we have carried out a separate experiment in the same geometry using a monochromatic γ source. The spectrum of the K edge is then freed from the contribution of characteristic x-ray photons and such a spectrum is used to determine the K shell parameters. Measured K shell parameters are compared with those obtained from FFAST tabulations.

2. Theory

When monochromatic x-ray beam of intensity I_o is incident on a target of thickness t, it may undergo various interactions with the target material, viz. Rayleigh scattering (elastic), Compton scattering (inelastic), photoelectric absorption and pair production (only if $h\nu \geq 1.022$ MeV). Due to these the x-ray beam gets attenuated and an intensity of I_t is transmitted through the target. The transmitted intensity, I_t, is observed as follows:

$$I_t = I_o e^{-(\mu/\rho)\rho t} \tag{1}$$

where μ/ρ is the total *mass attenuation coefficient*, ρ is the density and t is the thickness of the target. ρt is called as the mass thickness. μ/ρ depends on the incident x-ray energy and the target material. Hence, to say, it is constant for a given target at a given x-ray energy. It also represents the total attenuation cross-section (both scattering and absorption) when suitably multiplied with some constants. Rearranging the above equation we get

$$\frac{\mu}{\rho} = \frac{1}{\rho t} \ln\left(\frac{I_o}{I_t}\right). \tag{2}$$

Photoelectric parameters, such as the absorption edge energy, photoelectric cross-section at the edge energy, jump ratio, jump factor, Davisson–Kirchner ratio and oscillator strength, quantify the atomic electron photoelectric effect. The photoelectric cross-section, σ_{PE}, represents the probability of the photon to undergo photoelectric absorption. This depends on the energy of the photon and the state of the electron. This is like a resonance phenomenon. The cross-section will be zero if the photon energy is less than the atomic electron binding energy and maximum when the photon energy is exactly equal to the binding energy. Then it goes on decreasing rapidly with the increase in photon energy.

The total photon attenuation cross section, σ_T, for the material is related to the mass attenuation coefficient, μ/ρ, by

$$\sigma_T(E) = \frac{A}{N_o}\left(\frac{\mu}{\rho}\right) \tag{3}$$

where A is the atomic mass of the target atom and N_o is the Avogadro number. For photon of energy less than 1.022 MeV (no pair production)

$$\sigma_T = \sigma_{PE} + \sigma_{Coh} + \sigma_{Incoh}$$

where σ_{PE} is the photoelectric cross section, σ_{Coh} is the coherent (the Rayleigh) scattering cross section and σ_{Incoh} is the incoherent (the Compton) scattering cross section.

By measuring μ/ρ at various energies, the total cross-section σ_T can be calculated. A plot of σ_T versus energy E of photons gives a saw tooth structure at K shell binding energy of the target. The cross-section above the K edge is essentially due to involvement of K and higher shell electrons in photoelectric process and the scattering. The cross-section below the K edge is due to involvement of L and higher shell electrons in photoelectric process and the scattering. The cross section just above the K edge is

$$\sigma_a = \tau_K + \tau_L + \tau_M + \cdots + \sigma_{Coh} + \sigma_{Incoh}$$

and the cross section just below the K edge is

$$\sigma_b = \tau_L + \tau_M + \cdots + \sigma_{Coh} + \sigma_{Incoh}$$

where τ_K , τ_L and τ_M are the K, L and M shell photoelectric cross sections, respectively. In that very narrow energy interval, all the components remains constant, hence the difference

$$\sigma_a - \sigma_b = \tau_K \tag{4}$$

gives the K shell photoelectric cross-section at the K edge energy, which represents the maximum probability of photoelectric absorption by the K shell electron.

The K-shell jump ratio is the ratio of the cross section above the edge, σ_a, to the cross section just below the edge, σ_b, and it is given by

$$r_K = \frac{\sigma_a}{\sigma_b}. \tag{5}$$

The K shell absorption jump factor is the probability that a K shell electron will be ejected from the target element rather than any other shells. Neglecting the contribution of scattering which is very small compared to the photoelectric cross section at the edge, the K shell absorption jump factor J_K is related to the K shell absorption jump ratio r_K through the relation

$$J_K = \frac{\tau_K}{\tau_K + \tau_L + \tau_M + \cdots} \approx \frac{\sigma_a - \sigma_b}{\sigma_a} = \frac{r_K - 1}{r_K}. \tag{6}$$

The ratio of the total photoelectric cross section above the edge to the K-shell photoelectric cross section at K edge is known as the Davisson–Kirchner ratio and it is reciprocal of the K shell jump ratio J_K. It is given by

$$\text{Davisson–Kirchner ratio} = \frac{\sigma_{PE}^a}{\tau_K} = \frac{1}{J_K} \approx \frac{\sigma_a}{\sigma_a - \sigma_b}. \tag{7}$$

To determine these photoelectric parameters experimentally, generally one has to obtain μ/ρ values as a function of photon energy, E, around the K edge using x-ray absorption spectroscopy (XAS). Then the total cross-section values can be determined using Eq. (3). In the plot of E versus $\sigma_T(E)$, extrapolating the region above the K edge to meet the K edge energy gives σ_a and a similar extrapolation of the region below the K edge gives σ_b. Then by using above equations one can calculate the K shell photoelectric parameters. Different methods used to determine the K shell photoelectric parameters are briefly given in the following.

3. Experimental details

The experimental arrangement is as shown in Fig. 1. It comprises a beta source S, a converter foil C, a Perspex® absorber P, an elemental target T and a HPGe detector D coupled to 16 K multichannel analyzer. We have used $^{90}Sr \rightarrow {}^{90}Y$ radioactive source which emits beta particles with end point energies 546.2 keV and 2281 keV. The half life of ^{90}Sr is 28.4 years and that of ^{90}Y is 64 h. So the daughter nucleus ^{90}Y is in secular equilibrium with parent nucleus ^{90}Sr. Because of long half life of ^{90}Sr, the intensity of emitted beta particles remains constant throughout the experiment. The iron foil of thickness 86.57 mg/cm^2 is used as a converter to produce continuous external bremsstrahlung (EB) photons. It is well known that the intensity of EB is more for high Z materials. But, here we have used iron because the K x-ray photons of iron do not lie in the K edge energy region of the elements used in the present investigation. As the beta spectrum is

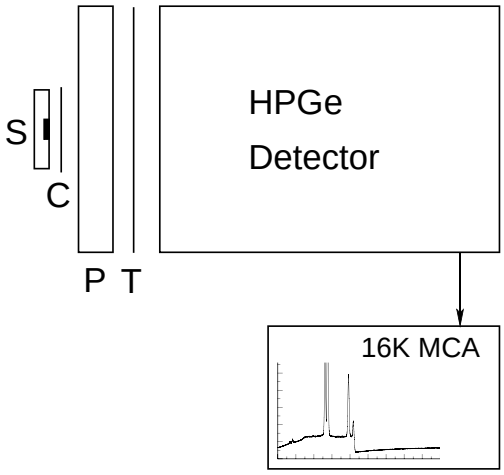

Fig. 1. Experimental arrangement.

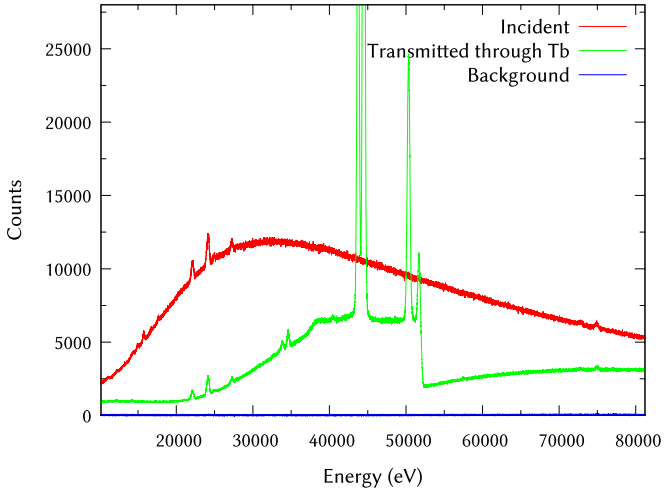

Fig. 2. Incident, transmitted and background spectrum for Tb target.

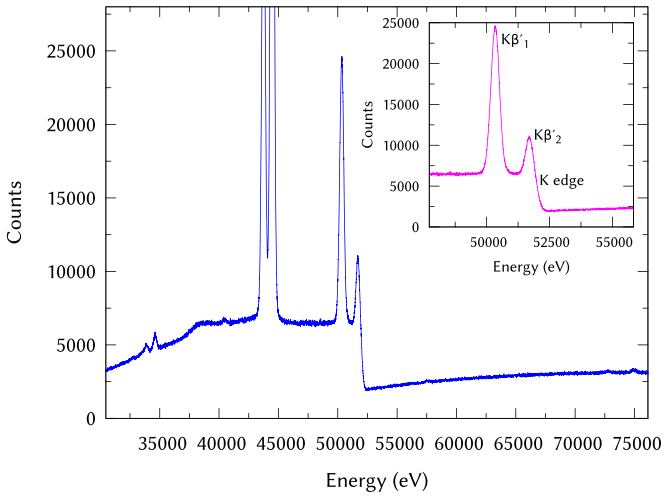

Fig. 3. Background corrected transmitted EB spectrum for Tb target.

continuous in energy distribution from 0 to 2281 keV, the high energy beta particles may transmit through the iron foil and consequently produce unwanted EB photons in the detector material. Hence, a Perspex sheet of thickness 10 mm is used to prevent the beta particles from reaching the detector material. The EB photons are passed through the elemental target T. We have used pure elemental foils of Tb and Ho, and these are obtained from ESPI Metals, Oregon. The thickness of Tb and Ho is 95.3 and 94.1 mg/cm^2, respectively. A Canberra make high resolution HPGe detector of type GL0510P is used to measure the x-rays. The detector has an active diameter of 25.2 mm, an active area of 500 mm^2 and a beryllium window of 0.15 mm thickness. The output of the detector is coupled to 16 K Canberra make multi-channel analyzer. The detector is calibrated using Kα_1 and Kα_2 x-ray photons of Ho (46,699.98 eV and 47,547.1 eV) excited by 59.537 keV gamma radiation from ^{241}Am and Hf (54,612 eV and 55,790.8 eV) and Ta (56,277.6 eV and 57,533.2 eV) (Deslattes et al., 2003) excited by 122.1 keV and 136.5 keV gamma radiation from ^{57}Co source. We have used these K x-ray photons as their energy lie around the K edge energy of the targets and also the solid state effects disappear for emission energies; Deslattes et al. (2003) have observed a good agreement between experimental and theoretical K x-ray values. The obtained least square fit calibration constant is 5.07 eV per channel. We have checked the peak position of 59.537 keV gamma photons before and after the experiment and found that there was no change in peak position even by one channel. This indicated that the whole system was stable throughout the experiment.

First we have recorded the background spectrum by placing all the radioactive sources far away from the detector. Then the spectrum of EB photons is recorded by placing the iron converter foil C in between the source S and the Perspex absorber P. Such recorded background spectrum and EB spectrum are shown in Fig. 2. From the EB spectrum we notice that above 30 keV the intensity decreases with increasing energy of EB photon in accordance with EB theory. However, below 30 keV, intensity decreases with decreasing energy which is essentially due to absorption of low energy EB photons by the Perspex absorber. We have used such an EB spectrum to measure the K shell binding energy of the target. Next we have placed the elemental Tb target in position T and recorded the transmitted EB spectrum. The background corrected transmitted the EB spectrum for Tb is shown in Fig. 3. From the spectrum we notice that there is a sudden decrease in intensity of EB photons around the 52 keV which is essentially due to involvement of the K shell electrons of the Tb target in photo-absorption process.

The energy corresponding to such sudden drop region is known as K absorption edge energy. The K edge energy is the energy required to lift a K shell electron to the lowest level of the unoccupied state. The vacancy so created in the K shell by the EB photons is filled by the electrons from the higher shells and consequently the characteristic K x-rays (Kα_2, Kα_1, Kβ_1' and Kβ_2') are observed just below the sudden drop region. Below the K edge, the intensity of transmitted EB photons is constant over a small energy interval which is attributed to involvement of L and higher shell electrons in photo-absorption process. It is also important to notice that because of finite energy resolution of the detector, the Kβ_2' and K edge are not well separated. In order to estimate the Kβ_2' contribution in the lower energy region of the K edge, we have carried a separate experiment using monoenergetic gamma photons. In this experiment, we have excited, in the same experimental arrangement, the K x-ray photons of Tb atom using 122.1 keV and 136.5 keV gamma photons from ^{57}Co gamma source. Such excited K x-ray spectrum of Tb is shown in Fig. 4 (b). From this figure we notice that the Kβ_1' and Kβ_2' are well separated. We have normalized this spectrum with Kβ_1' peak obtained with EB photons (Fig. 4(a)) and then subtracted the former from the latter. The subtracted spectrum is shown in Fig. 4 (c). Evidently, this spectrum over the region of our interest is free from Kβ_2' x-ray peak. We have used such Kβ_2' corrected spectrum

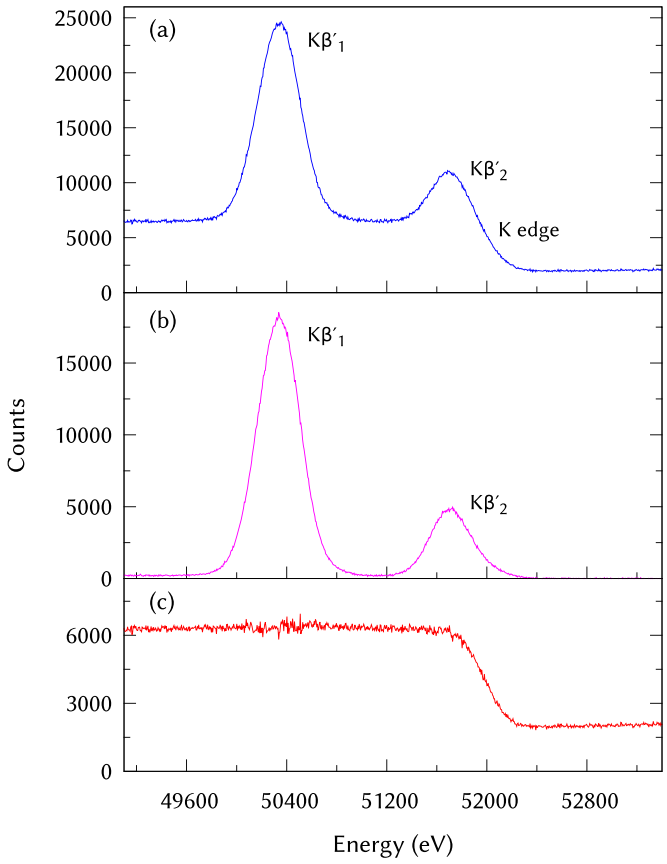

Fig. 4. $K\beta_1'$ and $K\beta_2'$ subtraction for Tb target.

for determining the K edge. Similarly we have also recorded the spectrum of EB photons transmitted through Ho elemental target and also corrected for $K\beta_2'$ contribution in the lower energy region of the sudden decrease portion. We have used such $K\beta_2'$ corrected spectrum for determining the K shell photoelectric parameters.

4. Analysis of the data

In order to determine the accurate value of K shell binding energy we have least square fitted the $K\beta_2'$ corrected transmitted data to the sigmoidal function of the type

$$I_t(E) = \frac{I_a - I_b}{1 + \exp\left(\frac{E - E_K}{dE}\right)} + I_b$$

where E is the energy corresponding to the transmitted EB photons, E_K is the K shell binding energy and dE is the change in energy E corresponding to the most significant change in intensity $I_t(E)$. I_a is the intensity corresponding to the lower energy branch and I_b is the intensity corresponding to the upper energy branch. The least squares fit sigmoidal function for the data of Tb is shown as a continuous curve in Fig. 5. From the figure we notice that the data fits well to this model. It is needless to say that the midpoint of this sigmoidal curve gives the K shell binding energy E_K of the Tb target atom. Similarly the least square fit sigmoidal function for data of Ho element is also shown as a continuous curve in Fig. 6. In order to represent the parameter E_K, we have taken the first derivative of the sigmoidal function which gives an inverted Gaussian like curve with well-defined minimum as shown in Fig. 7 for Tb and Ho. The minimum, which is the point of inflection

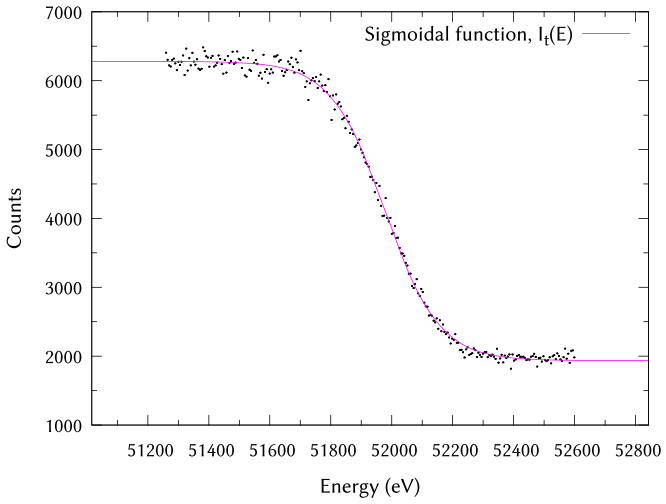

Fig. 5. Sigmoidal fit for K edge region of Tb.

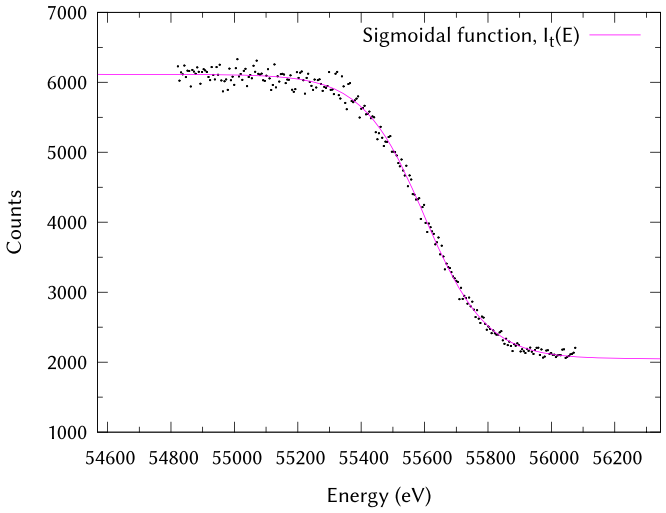

Fig. 6. Sigmoidal fit for K edge region of Ho.

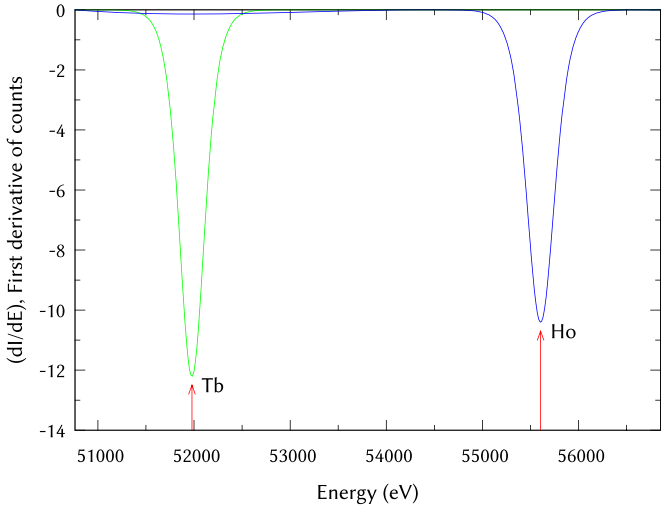

Fig. 7. First derivatives of sigmoidal fit curves for Tb and Ho targets.

in the steep fall, corresponds to the K edge of Tb and Ho atoms in the respective targets

The acquired incident and transmitted spectra need to be necessarily background corrected by subtracting them with the

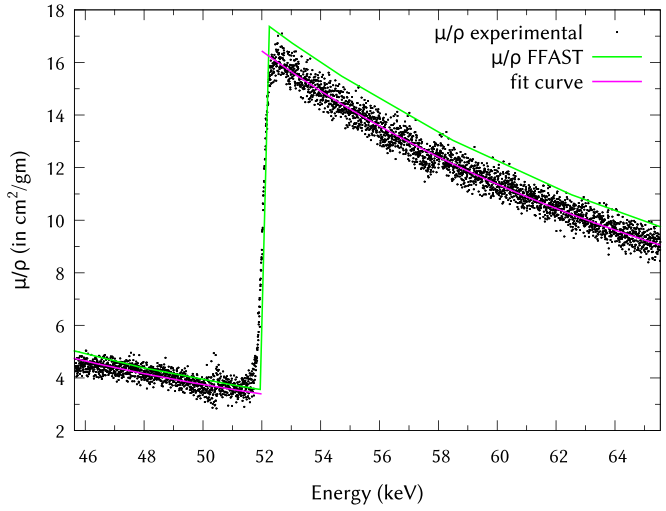

Fig. 8. Plot of μ/ρ as a function of energy for Tb along with the least square fit curves and the theoretical FFAST (Chantler et al., 2005) values.

acquired background spectrum. Then the mass attenuation coefficients around the K edge are calculated using Eq. (2) with 95.3 and 94.1 mg/cm^2 thickness, ρt, values for Tb and Ho targets, respectively. Here the incident and transmitted counts at an energy channel are taken as the respective incident and transmitted intensity at that particular energy. So each spectrometer channel provides intensity for one energy corresponding to it based on the calibration constant. Actually, the data requires deconvolution treatment to correlate the counts at various channels to the intensity at any particular energy (Ayala and Mainardi, 1996). But as the counts due to continuous bremsstrahlung are varying slowly with respect to the channels, the use of data as it is without deconvolution also gives fairly good values of the mass attenuation coefficients.

Calculated μ/ρ values as a function of energy around the K edge of Tb and Ho are plotted in Figs. 8 and 9, respectively. Due to the statistical distribution of the count rate the points in the plot are scattered. So the data below and above the K edge are separately least square fitted to the equation $\ln(\mu/\rho) = a_0 + a_1 \ln(E)$, where a_0 and a_1 are the fit parameters. This is equivalent to the linear fit of $\ln(E)$ vs. $\ln(\mu/\rho)$ data. The fit curves are shown in the same figures. This fitting is necessary to determine the K shell photoelectric parameters. It is because, due to the finite resolution of the detector, the K edge is a steep rise spanning about 100 channels. This makes direct pointing out of the attenuation coefficients just above and below the K edge energy impossible. For this, the fit curves are individually extrapolated to the K edge energies determined above. Separate extrapolation of the curves fitted to the data above and below the edge gives the attenuation coefficient just above and below the K edge energy respectively. The obtained mass attenuation coefficient values are fed into Eq. (3) to get the cross sections just above the K edge energy, σ_a, and below the K edge energy, σ_b. Once we have σ_a and σ_b, remaining K shell photoelectric parameters can be calculated using Eqs. (4)–(7). Gnuplot scripts are written and executed for curve fitting and calculations. Similarly, theoretical attenuation coefficients from FFAST (Chantler et al., 2005) database are fit and extrapolated to get the theoretical K shell photoelectric parameters.

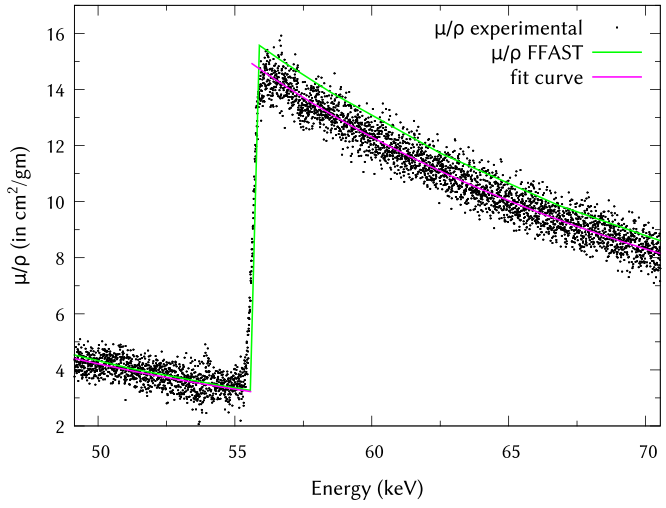

Fig. 9. Plot of μ/ρ as a function of energy for Ho along with the least square fit curves and the theoretical FFAST (Chantler et al., 2005) values.

5. Results and discussion

The K shell binding energy of Tb and Ho targets obtained by least square sigmoidal fit is presented in Table 1. These are the averages of five measurements. The error in the measured K edge values of Tb and Ho (Niranjana and Badiger, 2013) is 1 eV which is the standard deviation. Thus we see that even though the energy resolution of the detector for monoenergetic gamma rays at 59.537 keV is only about 300 eV, because of the use of continuous bremsstrahlung spectrum and possibility of fitting the experimental data to a sigmoidal function which has well-defined point of inflection, it is possible to determine the K shell binding energy of the atom with greater precision of ±1 eV. In Table 1 we have compared our measured values with the experimental values given by Deslattes et al. (2003) who have re-evaluated the K edge values from the values obtained by various investigators using the XPS method, which were earlier compiled by Bearden and Burr (1967). In the same table we have also compared our experimental values with the theoretical values given by Deslattes et al.; the theoretical values correspond to free atom. From the table we notice that the measured K absorption edge values differ with XPS values by just about 25 eV for Tb and about 16 eV for Ho.

The determined mass attenuation coefficients around the K edge of Tb and Ho along with the fit curve and the theoretical FFAST values are plotted in Figs. 8 and 9. The plots compare the determined attenuation coefficients with the theoretical FFAST values. From the plots it can be seen that, for both Tb and Ho, the measured values agree well with the FFAST values in the region below the K edge. But above the edge they are slightly less than the FFAST values. This is because the used foils do not meet the criteria (Creagh, 1987)

$$2 \leq \ln\left(\frac{I_0}{I_t}\right) \leq 4 \tag{8}$$

for energy region above the K edge. The foil thickness to be chosen for the experiment should meet the above condition to have experimental attenuation coefficients agreeing with the

Table 1
Comparison of measured K edge energy values of Tb and Ho with theoretical and other experimental values.

Element	Present experiment E_K (eV)	Theory[a] E_K (eV)	Other experiments[a] E_K (eV)
Tb	51,979 ± 1	51,999.5	52,003.8 ± 0.32
Ho	55,604 ± 1[b]	55,620.8	55,619.9 ± 0.37

[a] Deslattes et al. (2003).
[b] Niranjana and Badiger (2013).

Table 2
Comparison of measured K shell photoelectric parameters of Tb and Ho with theoretical FFAST (Chantler et al., 2005) values.

K shell PE	Tb		Ho	
parameters	Experimental	Theory[a]	Experimental	Theory[a]
τ_K (b/atom)	3446 ± 11	3722	3210 ± 8	3441
r_K	4.8 ± 0.2	4.984	4.66 ± 0.13 5.653[c]	4.863
J_K	0.79 ± 0.01 0.814 ± 0.05[b]	0.7994	0.785 ± 0.006 0.805 ± 0.05[b] 0.823 ± 0.039[c]	0.7944
D–K ratio	1.266 ± 0.015	1.251	1.27 ± 0.01	1.259

[a] FFAST (Chantler et al., 2005).
[b] Budak et al. (2003).
[c] Budak and Polat (2004).

theoretical values. As the cross section suddenly jumps at the K edge, one has to use two foils of different thickness; with one foil meeting Eq. (8) for below the edge region and the other for above the edge region.

The determined K shell photoelectric parameters of Tb and Ho are given in Table 2 along with those calculated from theoretical attenuation coefficient values from FFAST database and from other experimental values. The errors quoted are the uncertainties obtained from fitting and propagated to extrapolation and then to the K shell photoelectric parameters. The determined K shell photoelectric parameters from the present experiment for both Tb and Ho agree with the theoretical values; τ_K within 7%, r_K within 4%, J_K within 1% and the Davisson–Kirchner ratio within 1%. This shows that this simple and the novel method can be used to determine the K shell photoelectric parameters.

6. Conclusions

The present method determines the K shell photoelectric parameters of Tb and Ho using bremsstrahlung photons. The method involves a weak beta source, a weak gamma source, a single target and a high resolution HPGe detector. As this method is very simple all research laboratories can adapt this method for measuring the K shell photoelectric parameters of high Z elements.

Acknowledgments

The author N.M. Badiger would like to thank the Board of Research in Nuclear Science (BRNS), BARC, Mumbai, for sanctioning the research project. K.M. Niranjana would like to thank BRNS for awarding Junior Research Fellowship (JRF) in the research project.

References

Ayala, A.P., Mainardi, R.T., 1996. Measurement of the K X-ray absorption jump ratio of erbium by attenuation of a compton peak. Radiat. Phys. Chem. 47 (2), 177–181. http://dx.doi.org/10.1016/0969-806X(94)00189-Q, URL ⟨http://www.sciencedirect.com/science/article/pii/0969806X9400189Q⟩.

Bearden, J.A., Burr, A.F., 1967. Reevaluation of X-Ray Atomic Energy Levels. Rev. Mod. Phys. 39, 125–142. http://dx.doi.org/10.1103/RevModPhys.39.125, URL ⟨http://link.aps.org/doi/10.1103/RevModPhys.39.125⟩.

Bennal, A.S., Badiger, N.M., 2007. Measurement of K shell absorption and fluorescence parameters for the elements Mo, Ag, Cd, In and Sn using a weak gamma source. J. Phys. B: Atom. Mol. Opt. Phys. 40 (11), 2189, URL ⟨http://stacks.iop.org/0953-4075/40/i=11/a=019⟩.

Budak, G., Polat, R., 2004. Measurement of the K X-ray absorption jump factors and jump ratios of Gd, Dy, Ho and Er by attenuation of a Compton peak. J. Quant. Spectrosc. Radiat. Transf. 88 (4), 525–532. http://dx.doi.org/10.1016/j.jqsrt.2004.04.016, URL ⟨http://www.sciencedirect.com/science/article/pii/S0022407304001189⟩.

Budak, G., Karabulut, A., Ertugrul, M., 2003. Determination of K-shell absorption jump factor for some elements using EDXRF technique. Radiat. Meas. 37 (2), 103–107. http://dx.doi.org/10.1016/S1350-4487(02)00181-6, URL ⟨http://www.sciencedirect.com/science/article/pii/S1350448702001816⟩.

Çevik, U., Baltas, H., Çelik, A., Bacaksiz, E., 2006. Determination of attenuation coefficients, thicknesses and effective atomic numbers for $CuInSe_2$ semiconductor. Nucl. Instr. Methods Phys. Res. Sect. B: Beam Interact. Mater. Atoms 247 (2), http://dx.doi.org/10.1016/j.nimb.2006.01.064, URL ⟨http://www.sciencedirect.com/science/article/pii/S0168583X0600156X⟩.

Chantler, C.T., Olsen, K., Dragoset, R.A., Chang, J., Kishore, A.R., Kotochigova, S.A., Zucker, D.S., 2005. FFAST: X-Ray Form Factor, Attenuation and Scattering Tables (version 2.1). Technical Report, National Institute of Standards and Technology (NIST), Gaithersburg, MD. URL ⟨http://physics.nist.gov/ffast⟩.

Creagh, D.C., 1987. The resolution of discrepancies in tables of photon attenuation coefficients. Nucl. Instr. Methods Phys. Res. Sect. A: Accel. Spectrom. Detectors Assoc. Equip. 255 (1–2), 1–16. http://dx.doi.org/10.1016/0168-9002(87)91064-3, URL ⟨http://www.sciencedirect.com/science/article/pii/0168900287910643⟩.

Deslattes, R.D., Kessler, E.G., Indelicato, P., de Billy, L., Lindroth, E., Anton, J., 2003. X-ray transition energies: new approach to a comprehensive evaluation. Rev. Mod. Phys. 75, 35–99. http://dx.doi.org/10.1103/RevModPhys.75.35, URL ⟨http://link.aps.org/doi/10.1103/RevModPhys.75.35⟩.

Ertugrul, M., Karabulut, A., Budak, G., 2002. Measurement of the K shell absorption jump factor of some elements. Radiat. Phys. Chem. 64 (1), 1–3. http://dx.doi.org/10.1016/S0969-806X(01)00448-0, URL ⟨http://www.sciencedirect.com/science/article/pii/S0969806X01004480⟨.

Mallikarjuna, M.L., Gowda, S.B.A., Gowda, R., Umesh, T.K., 2002. Studies on photon interaction around the K-edge of some rare-earth elements. Radiat. Phys. Chem. 65 (3), 217–223. http://dx.doi.org/10.1016/S0969-806X(02)00260-8, URL ⟨http://www.sciencedirect.com/science/article/pii/S0969806X02002608⟩.

Nayak, S.V., Badiger, N.M., 2006a. A novel method for measuring K-shell photoelectric parameters of high-Z elements. J. Phys. B: Atom. Mol. Opt. Phys. 39 (12), 2893, URL ⟨http://stacks.iop.org/0953-4075/39/i=12/a=021⟩.

Nayak, S.V., Badiger, N.M., 2006b. Measurement of *K*-shell photoelectric absorption parameters of Hf, Ta, Au, and Pb by an alternative method using a weak β-particle source. Phys. Rev. A 73, 032707. http://dx.doi.org/10.1103/PhysRevA.73.032707, URL ⟨http://link.aps.org/doi/10.1103/PhysRevA.73.032707⟩.

Niranjana, K.M., Badiger, N.M., 2013. Determination of the K absorption edge energy of Ho in element and its compounds using the bremsstrahlung technique. J. Phys. B: Atom. Mol. Opt. Phys. 46 (9), 095006, URL ⟨http://stacks.iop.org/0953-4075/46/i=9/a=095006⟩.

Niranjana, K.M., Krishnananda, Badiger, N.M., Joseph, D., Kailas, S., 2013. Determination of K shell parameters of silver using high resolution HPGe detector spectrometer. Int. J. Nucl. Energy Sci. Technol. 7 (3), 179–190.

Niranjana, K.M., Krishnananda, Badiger, N.M., 2014. Effect of chemical environment on K shell binding energy of Ag and Sn. Chem. Phys. Lett. 604, 33–37.

Tran, C.Q., Chantler, C.T., Barnea, Z., de Jonge, M.D., Dhal, B.B., Chung, C.T.Y., Paterson, D., Wang, J., 2005. Measurement of the x-ray mass attenuation coefficient of silver using the x-ray-extended range technique. J. Phys. B: Atom. Mol. Opt. Phys. 38 (1), 89, URL ⟨http://stacks.iop.org/0953-4075/38/i=1/a=009⟩.